Diastereomeric DNA-Binding Geometries of Intercalated Ruthenium(II) Trischelates Probed by Linear Dichroism: $[Ru(phen)_2DPPZ]^{2+}$ and $[Ru(phen)_2BDPPZ]^{2+}$

Per Lincoln, Anders Broo, and Bengt Nordén*

Contribution from the Department of Physical Chemistry, Chalmers University of Technology, S-412 96 Gothenburg, Sweden

Received October 3, 1995[⊗]

Abstract: Linear dichroism (LD) has been used to probe the binding geometries of the diastereomeric adducts between DNA and the Δ and Λ enantiomers of $[Ru(phen)_2L]^{2+}$ where the chelate ligand L is either dipyrido[3,2-*a*:2′,3′-*c*]-phenazine (DPPZ) or its benzologue benzodipyrido[*a*:3,2-*h*:2′,3′-*j*]phenazine (BDPPZ). By combined use of LD and emission anisotropy excitation spectra measured in highly viscous solution the absorption envelope of the metal-to-ligand charge transfer (MLCT) region has been for the first time resolved in a complex of this type bound to DNA. The absorption can be described by four effective polarization directions (three almost orthogonal), along one of which any transition is polarized, assignments which are in good agreement with molecular orbital (INDO/S) calculations. The analysis of the LD spectrum provides the orientation of the complex in terms of several angles. Near perpendicularity relative to the DNA helix axis, found for the in-plane long and short axes of BDPPZ and DPPZ, together with extensive hypochromicity of the corresponding intraligand transitions, supports intercalation of the (B)DPPZ ligands between the DNA bases as earlier studies have indicated. MLCT transition moments that make an oblique angle to the molecular plane of the (B)DPPZ chromophores confirm this orientation and, in addition, provide strong evidence for a rotation (roll) of the complex around the pseudo-dyad axis. The roll is small (varying between 5 and 15°), but significant, and has *the same sign* (clockwise) for both enantiomeric forms of the two complexes studied and shows only minor variations between calf-thymus DNA and alternating GC or AT homopolymer duplexes. It may reflect a property intrinsic of DNA (tilt of bases) or be a result of steric interference of the two phenanthroline "propeller blades" with a groove. The roll provides the first example of an angle in a DNA system that has been determined with its sign from LD spectroscopy.

Introduction

The interaction of DNA with substitution-inert transition metal complexes has been an active area of research during the last decade.[1−6] Ruthenium oligopyridyl complexes in particular, due to a combination of easily constructed rigid chiral structures spanning all three spatial dimensions and a rich photophysical repertoire, have been useful for such diverse applications as probing the tertiary structure of nucleic acids[5,7−10] and binding and hybridization,[11,12] for achieving and probing photosensitized DNA cleavage,[13−15] and for probing DNA-mediated electron transfer.[16−18]

Despite a considerable amount of published material, however, our knowledge of the nature of the binding of these complexes to DNA and their binding geometries has remained relatively modest. The binding mode, intercalative or not, of the parent complex $[Ru(phen)_3]^{2+}$ is still a controversial issue.[19−22] On the other hand, there is a consensus about classical intercalative binding of the recently developed complexes, such as $[Ru(phen)_2DPPZ]^{2+}$, in which one of the phenanthrolines of the tris complex has been extended.[8,23a,24]

Early studies of complexes with DPPZ (dipyrido[3,2-*a*:2′,3′-*c*]phenazine)[23b] in $[Ru(bipy)_2DPPZ]^{2+}$ and $[Ru(phen)_2DPPZ]^{2+}$ had shown that the luminescence of the complexes was

[⊗] Abstract published in *Advance ACS Abstracts,* March 1, 1996.

(1) Nordén, B.; Lincoln, P.; Åkerman, B.; Tuite, E. DNA Interactions with Substitution-Inert Metal Ion Complexes. *Met. Ions Biol. Syst.* In press.
(2) Sigman, D. S.; Mazumder, A.; Perrin, D. M. *Chem. Rev.* **1993**, *93*, 2295.
(3) Pyle, A. M.; Barton, J. K. *Prog. Inorg. Chem.* **1990**, *38*, 413.
(4) Basile, L. A.; Barton, J. K. *Met. Ions Biol. Syst.* **1989**, *25*, 31.
(5) Chow, C. S.; Barton, J. K. *Meth. Enzymol.* **1992**, *212*, 219.
(6) Balzani, V.; Ballardini, R. *Photochem. Photobiol.* **1990**, *52*, 409. Juris, A.; Balzani, V.; Barigelletti, F.; Campagna, S.; Belser, P.; von Zelewsky, A. *Coord. Chem. Rev.* **1988**, *84*, 85.
(7) Barton, J. K.; Danishefsky, A. T.; Goldberg, J. M. *J. Am. Chem. Soc.* **1984**, *106*, 2172−2176.
(8) Friedman, A. E.; Kumar, C. V.; Turro, N. J.; Barton, J. K. *Nucleic Acids Res.* **1991**, *19*, 2595.
(9) Nordén, B.; Tjerneld, F. *FEBS Lett.* **1976**, *67*, 368.
(10) Barton, J. K.; Basile, L. A.; Danishefsky, A.; Alexandrescu, A. *Proc. Natl. Acad. Sci. U.S.A.* **1984**, *81*, 1961.
(11) Friedman, A. E.; Chambron, J.-C.; Sauvage, J.-P.; Turro, N. J.; Barton, J. K. *J. Am. Chem. Soc.* **1990**, *112*, 4960−4962.
(12) Jenkins, Y.; Barton, J. K. *J. Am. Chem. Soc.* **1992**, *114*, 8736.
(13) Kelly, J. M.; Tossi, A. B.; McConnell, D. J.; Oh Vigin, C. *Nucleic Acids Res.* **1985**, *13*, 6016−6034. Kelly, J. M.; McConnell, D. J.; Oh Vigin, C.; Tossi, A. B.; Kirsch-DeMesmaeker, A.; Masschellein, A.; Nasielski, J. *J. Chem. Soc., Chem. Commun.* **1987**, 1821−1823.
(14) Sentagne, C.; Chambron, J.-C.; Sauvage, J.-P.; Paillous, N. *J. Photochem. Photobiol. B: Biol.* **1994**, *26*, 165.
(15) Fleisher, M. B.; Waterman, K. C.; Turro, N. J.; Barton, J. K. *Inorg. Chem.* **1986**, *25*, 3549−3551.
(16) Murphy, C.; Arkin, M. R.; Jenkins, Y.; Ghatlia, N. D.; Bossman, S. H.; Turro, N. J.; Barton, J. K. *Science* **1993**, *262*, 1025.
(17) Murphy, C. J.; Arkin, M. R.; Ghatlia, N. D.; Bossmann, N. D.; Turro, N. J.; Barton, J. K. *Proc. Natl. Acad. Sci. U.S.A.* **1994**, *91*, 5315.
(18) Meade, T. J.; Kayyem, J. F. *Angew. Chem., Int. Ed. Engl.* **1995**, *34*, 352.
(19) Rehmann, J. P.; Barton, J. K. *Biochemistry* **1990**, *29*, 1701. Rehmann, J. P.; Barton, J. K. *Biochemistry* **1990**, *29*, 1710.
(20) Satyanarayana, S.; Dabrowiak, J. C.; Chaires, J. B. *Biochemistry* **1993**, *32*, 2573.
(21) Satyanarayana, S.; Dabrowiak, J. C.; Chaires, J. B. *Biochemistry* **1992**, *31*, 9319.
(22) (a) Eriksson, M.; Leijon, M.; Hiort, C.; Nordén, B.; Gräslund, A. *J. Am. Chem. Soc.* **1992**, *114*, 4933. (b) Eriksson, M.; Leijon, M.; Hiort, C.; Nordén, B.; Gräslund, A. *Biochemistry* **1994**, *33*, 5031.
(23) (a) Hiort, C.; Lincoln, P.; Nordén, B. *J. Am. Chem. Soc.* **1993**, *115*, 3448. (b) Dickeson, J. E.; Summers, L. A. *Aust. J. Chem.* **1970**, *23*, 1023.
(24) Haq, I.; Lincoln, P.; Suh, D.; Nordén, B.; Chowhry, B. Z.; Chaires, J. B. *J. Am. Chem. Soc.* **1995**, *117*, 4788−4796.

0002-7863/96/1518-2644$12.00/0

completely quenched in water solution but restored upon binding to DNA.[11,25] The affinity for DNA was found markedly larger compared to Ru(phen)$_3^{2+}$ (for [Ru(phen)$_2$DPPZ]$^{2+}$ binding constant $>10^6$ M^{-1} in 50 mM NaCl and 10^8 M^{-1} in 10 mM NaCl).[21,23a,24,26] If the DPPZ ligand is intercalated as both photophysical and thermodynamical properties indeed suggest, it is clear for steric reasons that the two ancillary ligands, whether phenanthroline or bipyridyl, should have quite different orientations relative to the DNA and therefore give rise to different properties for the two diastereomeric adducts formed from the Δ and Λ enantiomer. Studies on homochiral [Ru(phen)$_2$DPPZ]$^{2+}$ have shown that although the free energy of binding to DNA varies relatively little between the enantiomers,[24] there are great differences in luminescence intensities and lifetimes, the Δ enantiomer exhibiting a 6−10 times higher relative quantum yield than Λ when bound to DNA.[23a]

In order to understand in detail the origin of these diastereomeric effects we here use linear dichroism[27] to probe binding geometries of the DNA adducts of the Δ and Λ forms of [Ru(phen)$_2$DPPZ]$^{2+}$ and its benzologue [Ru(phen)$_2$BDPPZ]$^{2+}$ {BDPPZ = benzodiprido[*a*:3,2-*h*:2′,3′-*j*]phenazine}. Our structure analysis will refer to calf thymus DNA in the limit of very low binding ratios; however, measurements on [poly(dA-dT)]$_2$ and [poly(dG-dT)]$_2$ show only minor variations, indicating binding geometries that are essentially independent of base sequence.

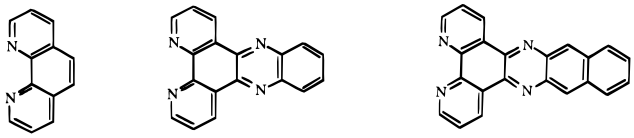

In earlier optical studies of DNA adducts with metal complexes the problem of overlapping absorption bands of different electronic transitions has generally been ignored.[28,29] Here we have used emission anisotropy spectra to resolve the spectral overlap between differently polarized transitions. We also address the problem by exploiting intraligand transitions to assess the orientation of the ligand in the DNA adduct. To gain further insight into the origin of overlapping absorption components and transition moment directions, we have finally carried out molecular orbital calculations on the Ru(phen)$_3^{2+}$ and Ru(phen)$_2$DPPZ^{2+} chromophores.

Another problem that we have been fortunate to circumvent in the present particular case of DNA−metal complex adducts is related to the fact that polarized absorption intensity is proportional to the cosine square of the angle that the transition moment makes with the electric field of light. For this reason linear dichroism cannot normally determine the sign of the angle at which a studied chromophore is inclined relative to the direction of preferred orientation (helix axis of DNA).[27] We find that the metal-to-ligand charge transfer (MLCT) transitions, responsible for the visible absorption of the ruthenium complexes, provide one strong absorption component which is polarized near 55° relative to the short in-plane axis of the extended (intercalated) ligand. This component is an independent, very sensitive, probe of any inclination of the short axis of the intercalated ligand and, furthermore, also an indicator of the *sign* of inclination. Our results indeed indicate that the ruthenium DPPZ/BDPPZ complexes are intercalated, but also that they all have a cognate deviation from the idealized B-DNA intercalative perpendicular binding geometry, characterized by a slight roll around the long axis of the intercalating ligand. Interestingly, the results indicate that the sense of roll is the same for opposite enantiomers suggesting that it reflects a property intrinsic of DNA (such as tilted basepairs) rather than diastereomeric interactions of the phenanthroline blades with a helical groove.

Experimental Section

Chemicals. Chemicals and solvents were of analytical grade and were used as received unless otherwise noted. All experiments were performed in a buffer of 10 mM NaCl/1 mM sodium cacodylate of pH 7 in triple deionized (Milli-Q) water. Calf thymus DNA, obtained from Sigma, was dissolved in buffer and filtered twice through a 0.8 μm Millipore filter. The synthesis of optically pure [Ru(phen)$_2$DPPZ]$^{2+}$ enantiomers from homochiral [Ru(phen)$_2$(1,10-phenanthroline-5,6-dione)](PF$_6$)$_2$ has been reported elsewhere,[23a] as has the synthesis of the DPPZ ligand.[23b]

The [Ru(phen)$_2$BDPPZ]$^{2+}$ enantiomers were synthesized by an analogous procedure with 2,3-diaminonaphthalene (used as received from Aldrich) in the condensation step. After chromatography of the hexafluorophosphate salt over Al_2O_3 with acetonitrile as eluent, the enantiomers were recrystallized from acetonitrile/ethanol. The anion was exchanged by precipitation with tetra-*n*-butylammonium bromide in acetone solution. The absorption spectrum in water solution was in good agreement with the published data for the racemic complex.[30] The BDPPZ ligand itself was synthesized analogously to DPPZ[23b] by condensation of 2,3-diaminonaphthalene with 1,10-phenanthroline-5,6-dione and recrystallized from xylene. Optically pure Λ-[Ru(phen)$_3$]$^{2+}$ was obtained by recrystallization of the sparingly soluble arsenyl-L-(+)-tartrate salt from dimethyl sulfoxide/water.

The circular dichroism (CD) spectrum of Λ-[Ru(phen)$_2$BDPPZ]$^{2+}$ is rather similar to that of the parent Λ-[Ru(phen)$_3$]$^{2+}$ in the MLCT bands (for CD of DPPZ complex see ref 23a). In the UV region, the expected decrease by about 2/3 of the phenanthroline exciton CD is observed: For Λ-(Ru(phen)$_2$BDPPZ)Br$_2$ in water, the wavelengths of maxima and troughs (in nm), with values of $\Delta\epsilon$/M^{-1} cm^{-1} given in parentheses, were 468 (+18), 417 (−20), 297 (+83), 267 (+324), 258 (−154), and corresponding data for Λ-(Ru(phen)$_3$)Cl$_2$ were 464 (+21), 418 (−15), 295 (+85), 267 (+625), 258 (−451).

Spectroscopy. Absorption, linear dichroism, and luminescence excitation spectra were all measured with a spectral band width of the incoming light of 2 nm. All spectra were recorded and stored as vectors with one intensity reading per nanometer wavelength. Isotropic absorption spectra were measured on a Cary 203 spectrophotometer in a 0.5-cm cell. The isotropic absorption spectrum will be treated as the sum of component absorption bands $\epsilon(\lambda)_i$ (absorbance as a function of wavelength for transition *i*) each with its characteristic polarization in the chromophore oordinate system:

$$A^{\mathrm{iso}}(\lambda) = \sum \epsilon(\lambda)_i \qquad (1)$$

(a) Emission Anisotropy. Samples of ruthenium complex−DNA solutions in buffer ([Ru] = 10 μM, phosphate/Ru = 50) were stirred with an excess of sucrose at 30° for several hours, undissolved sugar was removed by centrifugation, and the clear syrup was used immediately for the experiment. For temperatures down to −3 °C, excitation spectra were recorded on a Spex Fluorolog τ2 spectrofluorimeter, temperature controlled with a thermostated circulating bath. Spectra at lower temperatures were measured on an Aminco 500 spectrofluorimeter in a liquid nitrogen cryostat (Oxford Instruments). The emission was measured at 590 nm, with a slit width of 15 nm. Glan (calcite) polarizers were used for both the excitation and emission light in the Spex instrument, while in the Aminco instrument the emission polarizer was a Polaroid film polarizer.

(25) Jenkins, Y.; Friedman, A. E.; Turro, N. J.; Barton, J. K. *Biochemistry* **1992**, *31*, 10809−10816.

(26) (a) Kalsbeck, W. A.; Thorp, H. H. *J. Am. Chem. Soc.* **1993**, *115*, 7146. (b) Neyhart, G. A.; Grover, N.; Smith, S. R.; Kalsbeck, W. A.; Fairley, T. A.; Cory, M.; Thorp, H. H. *J. Am. Chem. Soc.* **1993**, *115*, 4423.

(27) Nordén, B.; Kubista, M.; Kurucsev, T. *Q. Rev. Biophys.* **1992**, *25*, 51. Nordén, B.; Kurucsev, T. *J. Mol. Recognit.* **1994**, *7*, 141.

(28) Hiort, C.; Nordén, B.; Rodger, A. *J. Am. Chem. Soc.* **1990**, *112*, 1971.

(29) Naing, K.; Takahashi, M.; Taniguchi, M.; Yamagishi, A. *J. Chem. Soc., Chem. Commun.* **1993**, 402.

(30) Hartshorn, R. M.; Barton, J. K. *J. Am. Chem. Soc.* **1992**, *114*, 5919.

The anisotropy of the emitted light as a function of excitation wavelength λ_{ex} was calculated as:[31]

$$EA(\lambda_{ex}) = (I_{VV} - I_{VH(c)})/(I_{VV} + 2I_{VH(c)}) \quad (2)$$

where I_{VH} is the excitation spectrum recorded with the excitation polarizer in the Vertical and the emission polarizer in the Horizontal position and so on. $I_{VH(c)}$ is the photomultiplier response-corrected excitation spectrum $I_{VH(c)} = I_{VH}(I_{HV}/I_{HH})$. For an immobile chromophore, the anisotropy for an electronic transition i is related to the angle χ_i between the absorbing and the emitting transition dipole moments according to:[31]

$$EA_i = (1/5)(3\cos^2\chi_i - 1) \quad (3)$$

The emission anisotropy over the absorption band originating from a single electronic (vibronic) transition is independent of excitation wavelength. However, the net anisotropy often shows wavelength dependence as a result of overlap of differently polarized transitions, being the average of anisotropies of the individual transitions weighted by their respective absorptions:

$$EA(\lambda_{ex}) = \sum(\epsilon(\lambda)_i EA_i)/\sum\epsilon(\lambda)_i \quad (4)$$

The emission anisotropy is a reduced dimensionless spectrum but may be transformed into a differential excitation spectrum (DE) by multiplication with the corresponding isotropic absorption spectrum:

$$DE(\lambda) = EA(\lambda)\sum\epsilon(\lambda)_i = \sum\epsilon(\lambda)_i EA_i \quad (5)$$

In the present case, for a chromophore with C_2 symmetry and with the emitting transition moment being A polarized (vide infra), the value EA_i will be +0.4 for A- and −0.2 for B-polarized transitions, respectively.

Linear Dichroism. The linear dichroism (LD) spectra of the ruthenium complexes in the presence of DNA in buffer ([Ru] = 40 μM, P/Ru = 30) were measured on a Jasco J-500 spectrodichrometer equipped and used as described elsewhere.[32−34] The DNA was oriented by a flow gradient of 1800 s^{-1} in a Couette cell with an outer rotating cylinder.[27] Samples were run in pairs with or without 10 μM of the intercalating dye methylene blue used as an internal orientation reference.[28] This dye has a strong absorption band at 675 nm, not overlapping with ruthenium-complex absorption, due to one purely long-axis polarized transition. The reduced linear dichroism was formed by dividing the linear dichroism with the isotropic absorbance:[27]

$$LD^r(\lambda) = LD(\lambda)/A(\lambda)^{iso} = (A(\lambda)^{parallel} - A(\lambda)^{perpendicular})/A(\lambda)^{iso} \quad (6)$$

The expression for the reduced linear dichroism of a single electronic transition in a uniaxially oriented sample is similar to that for the emission anisotropy:[27]

$$LD^r_i = (3/2)S(3\cos^2\theta_i - 1) \quad (7)$$

θ_i denoting the angle between the transition moment and the molecular orientation axis, in this case the helix axis of DNA. Just as for EA, LD^r for a single electronic transition is wavelength independent. The orientation factor S, with a value between 0 and 1, denotes the degree of orientation of DNA and is determined from the LD^r of the intercalated reference methylene blue, assuming it to be oriented perpendicular to the helix axis ($\theta = 90°$): i.e. $S = -LD^r(675\text{ nm})/1.5$. For overlapping transitions, the expression for the net $LD^r(\lambda)$ is also analogous to the corresponding one for the fluorescence anisotropy:[27]

$$LD^r(\lambda) = \sum(\epsilon(\lambda)_i LD^r_i)/\sum\epsilon(\lambda)_i \quad (8)$$

as is the expression for the corresponding differential spectrum:

$$LD(\lambda) = (A(\lambda)^{parallel} - A(\lambda)^{perpendicular}) = \sum\epsilon(\lambda)_i LD^r_i \quad (9)$$

(c) Resolution of Spectral Components. The isotropic absorption spectrum, normalized with regard to molar absorbance, $\sum\epsilon(\lambda)_i$, and the spectral profiles of the individual components $\epsilon(\lambda)_i$ are assumed constant for a given ruthenium-complex enantiomer bound to DNA under our conditions. The relation of the individual transitions to the experimental spectra can be expressed in matrix form:

$$\mathbf{E}C = \mathbf{S} \quad (10a)$$

Matrix **E** contains the individual absorption components $\epsilon(\lambda)_i$ and matrix **S** contains the experimental spectra $A^{iso}(\lambda)$, LD(λ), and DE(λ) (eqs 1, 5, and 9) as column vectors. The coefficient matrix **C** contains corresponding weights. As an example, we take a chromophore of C_{2v} symmetry in which electronic transitions are allowed only along three mutually perpendicular axes:

$$[\epsilon(\lambda)_x\ \epsilon(\lambda)_y\ \epsilon(\lambda)_z]\begin{pmatrix}1 & LD^r_x & EA_x\\ 1 & LD^r_y & EA_y\\ 1 & LD^r_z & EA_z\end{pmatrix} = [A^{iso}(\lambda)\quad LD(\lambda)\quad DE(\lambda)] \quad (10b)$$

Provided the coefficient matrix is non-singular the polarized absorption components $\epsilon(\lambda)_i$ are obtained by multiplying the inverse of the coefficient matrix with the matrix of the experimental spectra:

$$\mathbf{E} = \mathbf{S}\mathbf{C}^{-1} \quad (11)$$

Evidently, the maximum number of uniquely resolvable components is equal to the number of linearly independent experimental spectra.

Quantum Chemical Calculations. The absorption spectra and geometry of $[Ru(phen)_3]^{2+}$ and $[Ru(phen)_2DPPZ]^{2+}$ were calculated using the Intermediate Neglect of Differential Overlap (INDO)[35] model Hamiltonian (ZINDO program package[36]). A novel ruthenium parameter set was defined that could successfully predict both geometry and electronic spectra of a wide range of ruthenium complexes from $[Ru(NH_3)_6]^{2+}$ to $[Ru(NH_3)_5\text{-pyrazine-}Ru(NH_3)_5]^{4+/5+}$ (Broo and Lincoln, to be published). The geometry optimization of the $[Ru(phen)_3]^{2+}$ complex was started from a D_3 symmetric geometry. A very small deviation from D_3 symmetry was found in the final geometry due to the numerical procedure (D_3 symmetry cannot be enforced in the current implementation of the ZINDO program). The Ru−N bond distance for the $[Ru(phen)_3]^{2+}$ complex was predicted to be 2.054 Å. In the $[Ru(phen)_2DPPZ]^{2+}$ complex the Ru−N_{DPPZ} bond distances are predicted to be 2.055 Å and the Ru−N_{phen} distances to be 2.054 and 2.056 Å. The predicted Ru−N bond distances were in good agreement with the crystallographic Ru−N bond distance of 2.056 Å found for the $[Ru(bpy)_3]^{2+}$ complex (bpy = 2,2′-bipyridine).[37]

Results

Transition Moment Directions. In order to interpret the anisotropic absorption and excitation spectra of the ruthenium complex−DNA adducts in structural terms, we must first consider the assignments and transition moment directions of the electronic transitions involved. The strong broad absorption band centered at about 430 nm, which is responsible for the characteristic yellow-orange color of all ruthenium bipyridyl type complexes, is generally accepted to be due to several d → π^* metal-to-ligand charge transfer (MLCT) transitions, whereas the UV absorption is dominated by $\pi \rightarrow \pi^*$ intraligand (IL) transitions.[6,38a] $Ru(bipy)_3{}^{2+}$ oriented in single crystal host is

(31) Cantor, C. R.; Schimmel, P. R. *Biophysical Chemistry. Part II. Techniques for the Study of Biological Structure and Function*; W. H. Freeman and Co.: San Francisco, 1980.
(32) Nordén, B.; Davidsson, Å. *Tetrahedron Lett.* **1972**, *30*, 3093.
(33) Nordén, B.; Seth, S. *Appl. Spectrosc.* **1985**, *39*, 647−655.
(34) Nordén, B.; Tjerneld, F. *Chem. Phys. Lett.* **1977**, *50*, 508.
(35) Ridley, J. E.; Zerner, M. C. *Theor. Chim. Acta* **1973**, *32*, 111; **1976**, *42*, 223. Pople, J. A.; Beveridge, D. L.; Dobosh, P. A. *J. Chem. Phys.* **1967**, *47*, 2026.
(36) ZINDO: Zerner, M. C. Quantum Theory Project; University of Florida: Gainesville, FL 32611.
(37) Rillema, D. P.; Jones, D. S.; Levy, H. *J. Chem. Soc., Chem. Commun.* **1979**, 849.
(38) (a) Krausz, E.; Ferguson, J. *Prog. Inorg. Chem.* **1989**, *37*, 293. (b) Amouyal, E.; Homsi, A.; Chambron, J. C.; Sauvage, J. P. *J. Chem. Soc., Dalton Trans.* **1990**, 1841.

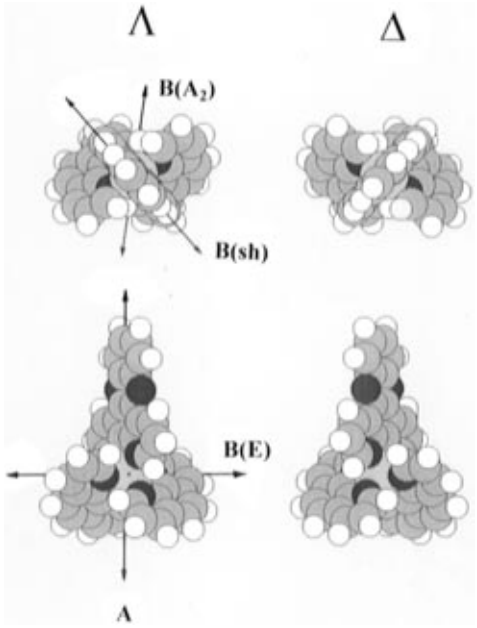

Figure 1. Pictures of the Λ and Δ enantiomers of [Ru(phen)$_2$DPPZ]$^{2+}$ viewed along the C_2 axis (top) as well as along the pseudo-C_3 axis. The four principal transition moment directions are shown: A and B(E) (both in the plane perpendicular to the pseudo-C_3 axis), B(A_2) (calculated to be slightly tilted relative to the pseudo-C_3 axis), and B(sh) (polarized along the short in-plane axis of the DPPZ ligand).

highly dichroic,[38a] the absorption in the visible as well as the emission being predominantly polarized (degenerately) in the plane containing the three 2-fold axes (irreducible representation E of point group D_3). A smaller fraction of the absorption, mainly on the blue side, is polarized along the 3-fold axis (A_2). The MLCT transitions of Ru(phen)$_3^{2+}$ have quite similar polarizations as evidenced from a comparison of emission anisotropy spectra for the bpy and phen complexes in rigid glass (results not shown). Apart from variations due to intraligand transitions of the DPPZ/BDPPZ ligands, only small differences are seen in energy and intensity in the normal absorption as well as circular dichroism spectra in the MLCT region when comparing [Ru(phen)$_3$]$^{2+}$ to [Ru(phen)$_2$DPPZ]$^{2+}$ and [Ru(phen)$_2$BDPPZ]$^{2+}$, indicating that the perturbation of the parent chromophore by the extension of one of the ligands is small. However, the symmetry lowering should break the degeneracy of the E transitions and lead to new transitions which, albeit close in energy, have orthogonal polarizations. The transitions of the resulting C_2-symmetric chromophore are polarized either along the 2-fold axis (irreducible representation A of point group C_2) or in a direction in the plane perpendicular to this axis (B). Assuming a conserved intensity in the original "E plane" (weak perturbation) this will lead to the two transitions A and B(E) polarized perpendicular to the original C_3 axis as shown in Figure 1. Correspondingly the A_2 transition in D_3 should remain polarized parallel to the original C_3 axis. In addition, short axis polarized transitions at low energy of the new extended ligand will constitute a fourth polarization direction denoted B(sh).

The INDO/S calculations on [Ru(phen)$_2$DPPZ]$^{2+}$ and [Ru(phen)]$_3^{2+}$ complexes support this conclusion (Table 1). The calculations indicate four major transition moment directions for the [Ru(phen)$_2$DPPZ]$^{2+}$ complex. These directions (depicted in Figure 1), consistent with directions expected for a small perturbation of the D_3 chromophore, will be used to resolve the absorption envelopes of the DPPZ and BDPPZ ruthenium−DNA adducts into polarized components (vide infra).

Figure 2 shows the reduced linear dichroism (LD^r) measured on DPPZ as well as on the [Ru(phen)$_2$DPPZ]$^{2+}$ complex in anisotropic hosts of stretched poly(vinyl alcohol). It is concluded that the first strong IL band at 372 nm in DPPZ is almost purely polarized along the long axis of this ligand, which in the metal complex coincides with the C_2-symmetry long axis, i.e. having A polarization. A corresponding polarization is found for the first two strong IL bands at 420 and 315 nm in the BDPPZ absorption spectrum (Figure 3b, LD and EA spectra not shown). Figure 2b also shows the emission anisotropy for [Ru(phen)$_2$DPPZ]$^{2+}$ immobilized in 1,2-propanediol glass at −70 °C and in isotropic poly(vinyl alcohol) film at room temperature. The overall similarity of the LD^r and EA curves indicates that the emission of this complex is also A polarized. The fact that the anisotropy is unchanged in the temperature range −75 to +25 °C suggests that a single excited state is responsible for the emission, not unexpected as the excited electron of the lowest MLCT state of [Ru(bpy)$_2$DPPZ]$^{2+}$ has been shown to be localized on the DPPZ ligand.[38b] The EA data enable us to resolve the isotropic absorption of the free complex into A and total B components as shown in Figure 2b. Below further information about the absorption components of different polarizations within the B group will be extracted from flow LD and emission anisotropy of the metal complexes when bound to DNA.

Absorption and Linear Dichroism Spectra. Isotropic absorption spectra of the two sets of enantiomers bound to DNA are shown in Figure 3, together with the spectra of the free complexes in buffer. The spectral effects of the DNA binding are on the whole similar for all four compounds, with remarkable hypochromic effects on the 372- and 315-nm IL bands for the DPPZ and BDPPZ complexes (hypochromicities of 50−70%). There are, however, small but significant differences between the Δ and Λ enantiomers in both sets of complexes. Most notable is the stronger hypochromism of the MLCT band for the Δ enantiomers, in contrast to the very slight difference in red shifts and hypochromisms of the IL bands between the enantiomers.

Linear dichroism spectra of [Ru(phen)$_2$DPPZ]$^{2+}$ and [Ru(phen)$_2$BDPPZ]$^{2+}$ enantiomers oriented by binding to flow-oriented DNA are also shown in Figure 3. The orientation factor (S in eq 7) was determined by running identical samples containing a small quantity of the intercalating dye methylene blue as an internal reference.[28,39] This dye, bound to DNA alone, has a somewhat more negative LD^r in the long-wavelength band than the DNA base absorption at 258 nm and was accordingly defined to have an LD^r value of $-1.5S$.[39] The simultaneous binding of the dye and ruthenium complex to DNA in the present proportions was not accompanied by any noticable changes in their respective absorption spectra or any other indications of mutual chromophoric interactions. The magnitude of the LD^r of the dye increased somewhat in the prescence of the ruthenium complexes indicating a slight increase in the orientation of the DNA. This effect was barely noticeable for the Δ enantiomers, while the increase in S was about 15% for the Λ enantiomers at a P/Ru ratio of 10.

The LD^r spectra calculated by dividing LD with the isotropic absorption are shown in Figure 4. The strongly negative LD^r for the IL BDPPZ band at 320 nm clearly supports a geometry with the 2-fold axis of this complex nearly perpendicular to the DNA helix axis for both enantiomers. A negative LD^r of almost the same magnitude in the long-wavelength tail of the MLCT band confirms the presence of a transition with A polarization also at this position in the spectrum.

Emission Anisotropy. The absorption spectrum of [Ru(phen)$_2$DPPZ]$^{2+}$ in the presence of DNA in buffer did not change significantly upon the addition of sucrose, nor did the shape of the excitation spectra change upon cooling this syrup-

(39) Tuite, E.; Nordén, B. *J. Am. Chem. Soc.* **1994**, *116*, 7548.

Table 1. Electronic Transitions of $[Ru(phen)_3]^{2+}$ and $[Ru(phen)_2DPPZ]^{2+}$ According to the INDO/S Calculations[a]

$Ru(phen)_3$					$Ru(phen)_2DPPZ$						
calculated			experiment[b]		calculated					experiment	
E ($\times 10^3$ cm^{-1})	f	D_3	E ($\times 10^3$ cm^{-1})	$\epsilon/10^3$	E ($\times 10^3$ cm^{-1})	f	C_2	polarization[d]	assignment[e]	E ($\times 10^3$ cm^{-1})	$\epsilon/10^3$
19.7	0.17	E			19.6	0.17	A		ML	21.6	
					19.7	0.12	B (E)	56°	ML	22.3	
20.1	0.24	E	22.3	18.4	20.0	0.17	A		ML	23.3	20.0[f]
					20.2	0.09	B (E)	56°	ML		
24.3	0.51	E	23.7	17.6	24.2	0.21	B (E)	54°	ML	23.8	
					24.3	0.05	B	86°	ML		
24.8	0.16	A_2			24.6	0.1	B (A_2)	−54°	ML	26.6	
					25.5	0.25	A		ML		
					27.0	0.22	A		IL	27.0	21.8
					27.4	0.13	B (sh)	3°	IL		
					33.2	0.23	B (sh)	5°	IL		
					33.6	1.17	A		IL	35.5	
					33.6	0.11	A		IL		
					36.6	0.06	B		mix		
					36.6	0.29	A		IL		
					37.1	0.16	A		IL	37.1	
37.0	0.90	E			37.2	0.14	A		ML		
					37.3	0.3	B	86°	ML		
					37.8	0.09	B		IL		
					38.2	0.05	A		IL		
38.7	1.86	A_2	38.2	112	38.8	1.42	B (A_2)	−42°	IL	37.7	117

[a] Calculated energies (E), oscillator strengths (f) and polarizations symmetries in point group D_3 or C_2. For classifications of B transitions, see text. Only transitions with calculated oscillator strengths >0.05 are included. [b] Reference 45. [c] Assignment from emission anisotropy (Figure 2b). [d] Angle between the transition moment and the y axis (the in-plane short-axis of DPPZ). Coordinate system chosen so that the x-axis is a 2-fold axis and the y axis lies in the plane of the ligand (e.g. DPPZ) containing the x axis. For $Ru(phen)_3$ in C_2 point group, polarization A_2 or D_3 becomes B (−35°) and the degenerate E polarization splits into B (55°) and A. [e] Transitions characterized as predominately metal-to-ligand (ML), intraligand $\pi \rightarrow \pi^*$ (IL), or a mixture of both (mix). [f] Reference 23 (extinction coefficients in water solution).

like solution to below 0 °C. The luminescence intensity, however, increased considerably at lower temperature. The value of the anisotropy, with maximum at 480 nm, increased with decreasing temperature to reach plateau values at +5 °C for the Λ enantiomer and −25 °C for the Δ enantiomer. As shown in Figure 4a the spectral profiles of the anisotropy for the two enantiomers are rather similar, and a resolution of the corresponding absorption spectra into A and B polarized absorption envelopes indicates that the difference in the absorption spectra is almost entirely due to the A (C_2-axis polarized) component. An interesting observation, which will prove quite helpful, is the near mirror symmetry relation between the LD^r of the Δ enantiomer and the anisotropy curve (Figure 4a). This demonstrates that the A transitions, which show the most positive anisotropy, are also those which exhibit the most negative LD^r.

To investigate whether the chromophores were really immobile on the time scale of luminescence lifetimes, when bound to DNA in the cold sucrose syrup, the anisotropy curve of DNA-bound Λ enantiomer in a 1:2 buffer/1,2-ethanediol rigid glass at −100 °C was measured. It was found perfectly superimposable upon the anisotropy curve recorded in sucrose syrup at −3 °C, except for a slightly increased structure due to narrowing of the bandwidth. Binding of the ruthenium complex to DNA in the ethanediol mixture at room temperature gave absorption spectral changes, as well as luminescence increase, very similar to those found with DNA in pure buffer solution.

$[Ru(phen)_2BDPPZ]^{2+}$ has previously been reported to be luminescent in water solution and to show only a modest further increase in quantum yield upon binding to DNA.[30] By contrast, our sample of the complex was found to have only a very weak luminescence whether in water or acetonitrile or when bound to DNA. Excitation spectra recorded on these weakly luminescent solutions did not show the characteristic BDPPZ absorption profile (most notably the 315-nm band was completely absent). Therefore, we conclude that $[Ru(phen)_2BDPPZ]^{2+}$ is virtually nonluminescent under these conditions and that the previously reported luminescence is likely to be due to impurities.

Resolution of Absorption Spectra in Polarized Components. Following the procedure described in the Experimental Section, the flow linear dichroism spectra of the metal complexes bound to DNA combined with the emission anisotropy data have been exploited to deconvolute the isotropic absorption spectra into four principal components as shown in Figure 5. A prerequisite for the analysis is that upon interaction with DNA the two enantiomers can still be considered the same chromophore. This assumption is justified by the quite small variation in the absorption spectra between the DNA adducts of the enantiomeric forms. This assumption also makes the interpretation of the LD spectra simple: the different LD spectra for the enantiomers of either complex can be interpreted only in terms of different angular orientations.

The LD^r_i values of the A polarized transitions were determined in two different ways for the DPPZ and BDPPZ complexes: either by searching for linear combinations of absorption and LD spectra in which the 320-nm BDPPZ transition vanished (TEM method),[40] or by scaling the LD^r curve to fit the FA curve for the Δ-DPPZ complex.[27] These methods gave similar LD^r values of -2.0 ± 0.2, although considerably more negative than the expected limiting −1.5. This deviation suggests that the long axis of the internal orientation standard methylene blue is somewhat inclined (by 15−20°) from exact perpendicularity to the DNA helix axis in agreement with earlier observations.[27] Therefore, the value of θ_A, the angle between the 2-fold axis of the metal complex and the helix axis, was taken equal to 90° for all four compounds, and the LD spectra accordingly rescaled.

Note the virtual mirror symmetry between the EA and LD^r curves above 350 nm for Δ-$[Ru(phen)_2DPPZ]^{2+}$ (Figure 4a) which indicates that the LD^r values for the transitions B(A_2) and B(E) are nearly identical and approximately equal to $-1/2$

(40) Michl, J.; Thulstrup, E. *Spectroscopy with Polarized Light*; VCH Publishers: New York, 1986; p 120.

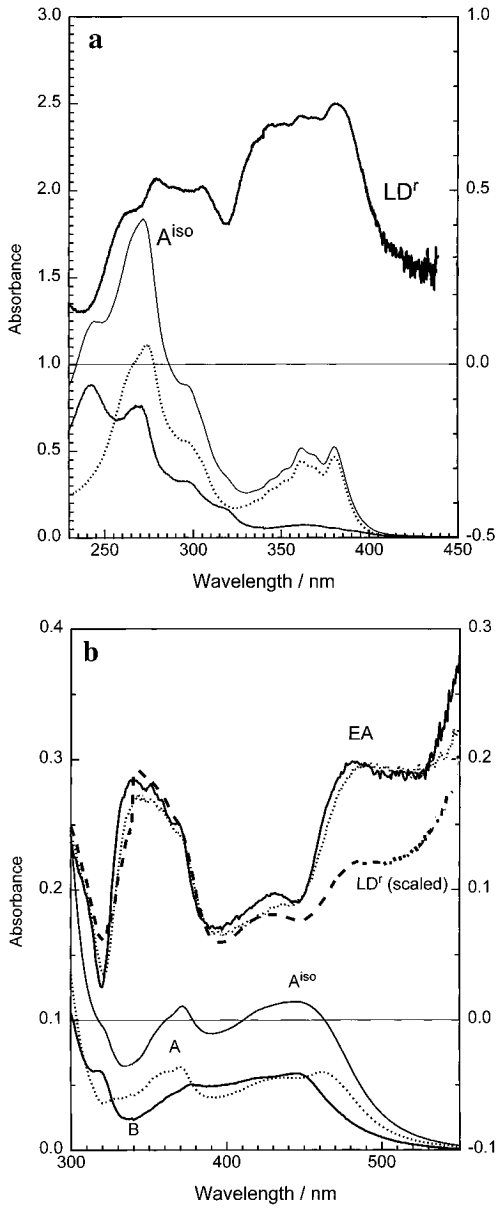

Figure 2. (a) Reduced linear dichroism (LD^r) of the DPPZ ligand oriented in stretched poly(vinyl alcohol) film and the corresponding isotropic absorption spectrum (A^{iso}). The latter is resolved into long-axis (dotted curve) and short-axis (solid curve) in-plane polarized components using the TEM method.[40] (b) Top: Emission anisotropy (EA) as a function of excitation wavelength for [Ru(phen)$_2$DPPZ]Cl$_2$ in propylene glycol glass at −75 °C (dotted curve) and in isotropic poly(vinyl alcohol) film at 25 °C (solid curve). Also shown is the reduced linear dichroism (LD^r) spectra (dashed curve) of the same compound in a stretched film of poly(vinyl alcohol); the LD^r is scaled by a factor of 0.4 to facilitate comparison with EA. The overall similarity of EA to LD^r shows that the emitting transition moment coincides with the preferred orientation axis of the complex in the stretched film. Bottom: Corresponding isotropic absorption spectrum resolved (using the EA data) into A and B polarized absorption envelopes.

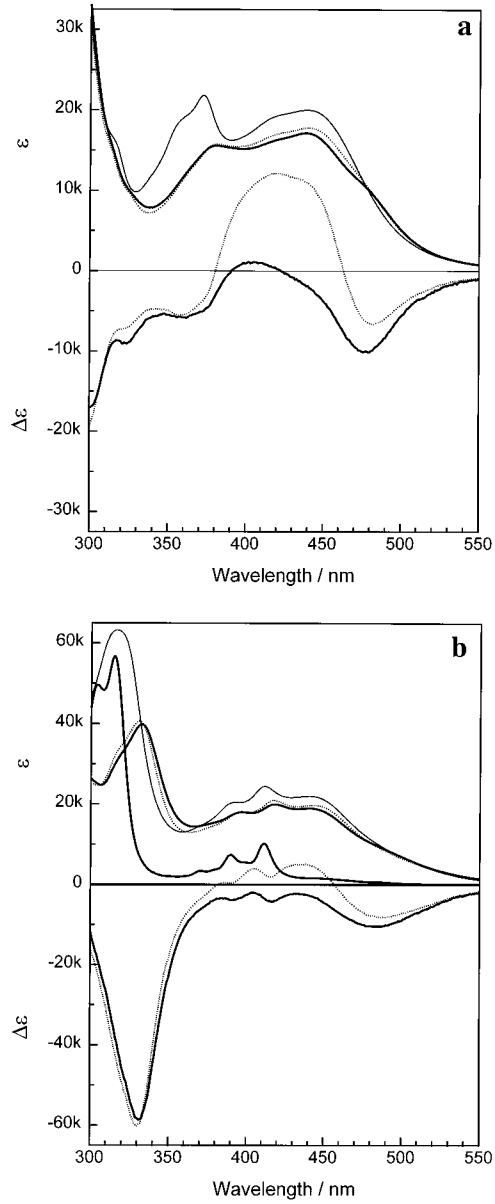

Figure 3. Isotropic absorption spectra (top) and flow linear dichroism spectra (bottom) of (a) [Ru(phen)$_2$DPPZ]$^{2+}$ and (b) [Ru(phen)$_2$BDPPZ]$^{2+}$: free (thin solid curve) and bound to DNA at a phosphate/complex ratio of 30 (Δ enantiomer: thick solid curve, Λ enantiomer: dotted curve). Also shown in (b) is the absorption spectrum of the free BDPPZ ligand in ethanol solution (structured thick solid curve).

of LD^r for the A-polarized transitions for this particular enantiomer. The slight displacement of the line of symmetry from the zero line corresponds to both LD^r B(E) and LD^r B(A$_2$) being smaller than 0.75, and a fit of the curves estimated the angle between the B(E) and B(A$_2$) polarization directions to be approximately 80°, which is smaller than the orthogonal arrangement expected for an unperturbed D_3 chromophore but slightly larger than the 70 °C predicted by the quantum mechanical calculation (Table 1). At 325 nm both curves exhibit a negative peak indicating the presence of a B-polarized transition that is nearly perpendicular to the helix axis. This feature is assigned to the intraligand DPPZ in-plane short-axis polarized transition, B(sh), observed at this wavelength in the linear dichroism spectrum of the ligand itself in stretched films (Figure 2a) and also predicted at this energy by the INDO/S calculation (Table 1).

The LD^r values of the **C** matrix (eqs 10 and 11) were calculated according to eq 7, with $\theta_{B(E)}$ as the unknown variable: $\theta_A = 90°$, $\theta_{B(A2)} = \theta_{B(E)} \pm 80°$, $\theta_{B(sh)} = \theta_{B(E)} \mp 50°$ (the first sign referring to the Λ enantiomer, see Figure 1). For the BDPPZ complex, the two pairs of absorption and linear dichroism spectra of the enantiomers in the presence of DNA form a basis set of experimental spectra. As the largest diastereomeric difference was anticipated to appear in the A-polarized absorption, the basis was resolved into one separate A component for each of the two enantiomers and two common components of, respectively, B(E) and B(A$_2$) polarization. In the final resolution (Figure 5a), any B(sh)-polarized absorption is effectively contained in the A-component

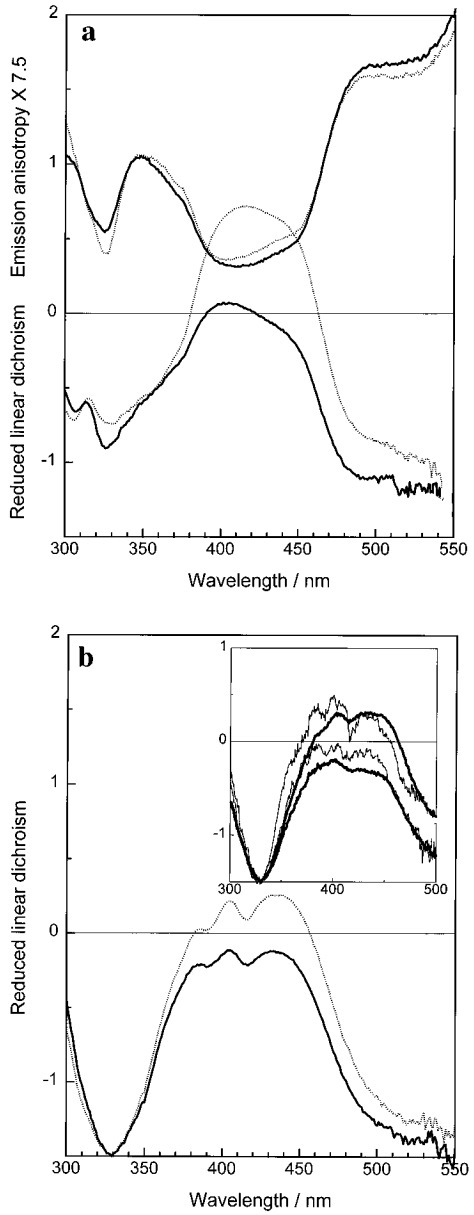

Figure 4. Reduced linear dichroism (LD^r, at bottom) and (for the DPPZ complexes) emission anisotropy (EA, at top) of the DNA adducts with the enantiomeric forms of the (a) $Ru(phen)_2DPPZ^{2+}$ and (b) $Ru(phen)_2$-$BDPPZ^{2+}$ complexes: Δ shown with solid curves and Λ with dotted curves. To facilitate comparison with LD^r the EA data have been scaled to give the same limiting values as LD^r (i.e. −0.2 in EA is scaled to −1.5). Inset in (b) shows LD^r of Δ- and Λ-$[Ru(phen)_2BDPPZ]^{2+}$ bound to alternating homopolymer duplexes $[poly(dG\text{-}dC)]_2$ (thick lines) and $[poly(dA\text{-}dT)]_2$ (thin lines) at a P/Ru ratio of 15.

absorption envelope since the value of $\theta_{B(E)}$ indicates that $\theta_{B(sh)}$ is close to 90°. For the DPPZ complex the differential excitation spectra (DE, eq 5) allows the resolution of more components: B(sh) as well as A components for both of the enantiomers.

Using trial values of $\theta_{B(E)}$, the coefficient matrix **C** was computed, inverted, and multiplied with the matrix of the corresponding basis of experimental spectra (eqs 10 and 11) to give the resolved absorption components which then could be examined. The resolved absorption components are shown in Figure 5, and the $\theta_{B(E)}$ values are given in Table 2. Comparison of the components resolved for the Δ and Λ enantiomers of $Ru(phen)_2DPPZ^{2+}$ (Figure 5, b and c) gives an idea about the significance of the analysis. A small variation between the MLCT A components between the Δ and Λ complexes can be related to different hypochromicities upon interaction with the

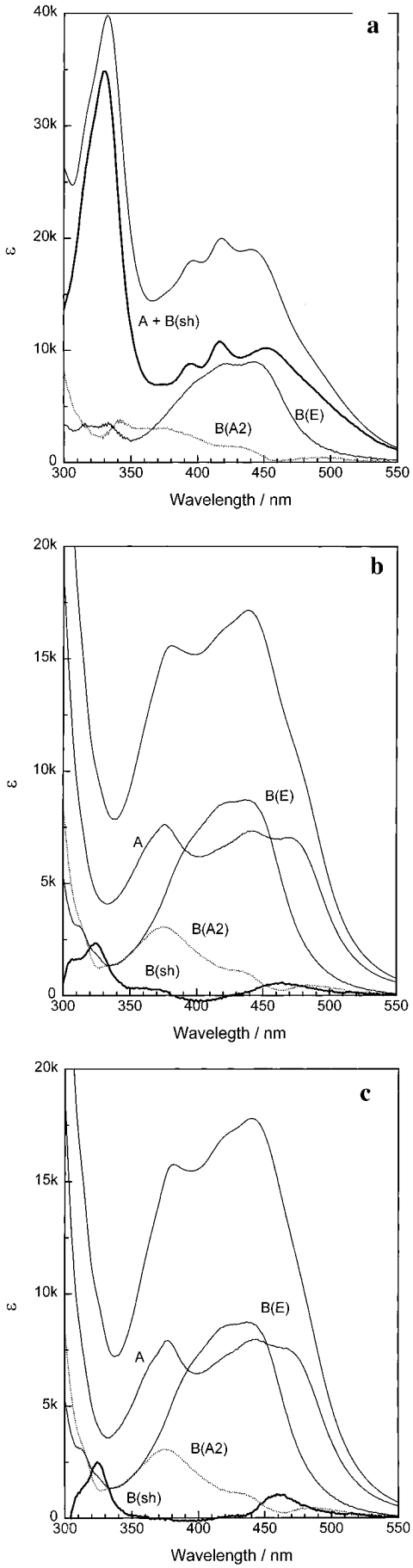

Figure 5. Resolved polarized absorption components (from eq 11) for DNA adducts of Δ-$[Ru(phen)_2BDPPZ]^{2+}$ (a) and Δ- and Λ-$[Ru$-$(phen)_2DPPZ]^{2+}$ (b and c). Corresponding geometric parameters are presented in Table 2 (notations of polarization directions according to Figure 1; top thin curves are isotropic absorption spectra).

Table 2. Angular Parameters of [Ru(phen)$_2$(L)]$^{2+}$ Enantiomers Bound to DNA[a]

	Δ (deg)		Λ (deg)	
L	$\theta_{B(E)}$	β	$\theta_{B(E)}$	β
DPPZ				
ct-DNA	+42	+7	−22	+13
BDPPZ				
ct-DNA	+40	+5	−28	+7
GC[b]	+47	+12	−25	+10

[a] $\theta_{B(E)}$ = angle between helix axis and B(E) transitions; β = roll angle as defined in the text. Uncertainties in angles are approximately ±3° for Δ and ±5° for Λ enantiomers. [b] For AT the short contour length of our sample led to a poor orientation and, hence, noisy LD spectra (see inset of Figure 3b). However, from the similar curve shapes roughly the same binding geomtries as for ct-DNA can be concluded.

DNA. As expected, the B(sh) component, by nature of it being a residual, shows a relatively large uncertainty.

The sign ambiguity of $\theta_{B(E)}$, originating from the cos^2 dependence of eq 7, could be solved since only one sign could be consistent with a negative LD^r of B(sh) and a geometry in which the extended ligand is pointing in toward the DNA. The latter orientation of DPPZ (and BDPPZ), in contrast to geometries in which the ligand is directed away from DNA, is obvious from the extensive hypochromism observed for its IL transitions indicating a close contact with the nucleo-bases. Furthermore, as the 2-fold axis of the intercalating ligand was found to be perpendicular to the helix axis, one may conveniently describe the deviation from "ideal" intercalative geometry as a roll around the 2-fold axis. The roll angle β is defined as a clockwise rotation (when viewed from ligand toward DNA) of the molecular plane of the intercalating ligand from the plane perpendicular to the helix axis. As expected (Table 2) generally no large deviations (5−13°) from the perpendicular geometry are found. A near perpendicular orientation is a prerequisite for an intercalation geometry and also consistent with earlier binding and viscosity data for Ru(phen)$_2$DPPZ^{2+} which suggests that this complex is intercalated.[24] The most striking feature, however, is the observation of exclusively *positive* values of roll angle with small variations between the enantiomeric forms of the complexes and between DNA and the two homopolymers.

Discussion

No detailed three-dimensional structure has yet been solved for a chiral metal complex bound to a DNA fragment but the present spectroscopic evidence, supported by earlier thermodynamic results, allows several conclusions to be drawn about binding geometries of both enantiomeric forms of the [Ru(phen)$_2$(DPPZ)]$^{2+}$ and [Ru(phen)$_2$(DPPZ)]$^{2+}$ complexes. While LD allows us to characterize the DNA binding geometry in terms of several angular parameters, other methods are required to settle whether the metal complex ions bind via the minor or the major groove. In a recent NMR study the Barton group detect an NOE between protons on the DPPZ ligand, located close to the center of the [Ru(phen)$_2$DPPZ]$^{2+}$ complex, and an aromatic base proton facing the major groove,[41] which could indicate major groove location at least for the particular hexanucleotide studied. By contrast, recent observations in our laboratory of virtually unaffected binding of [Ru(phen)$_2$DPPZ]$^{2+}$ to major-groove-glucosylated T4 DNA compared to CT-DNA (Tuite et al. to be published) as well as to the poly(dA)·[poly(dT)$_2$] triplex (Kim et al. to be published) suggests instead a location in the minor groove. In the present study, however, we shall leave the question about preferred groove open.

Large Chelate Wing Is Intercalated. It is beyond any doubt that the large BDPPZ (and DPPZ) chelate wing is intercalated between the DNA bases. The most direct evidence for this conclusion is the near coplanarity with the DNA bases, following from strongly negative LD^r values for transitions polarized both along the long and short in-plane axes of these ligands, supplemented with the strong hypochromicity of the intraligand absorption implying interaction with the nucleobase chromophores. The latter observation excludes an orientation of the complex in which the large ligand is instead pointing away from DNA. That [Ru(phen)$_2$(DPPZ)]$^{2+}$, in contrast to the parent [Ru(phen)$_3$]$^{2+}$,[20,21] is intercalated has also been inferred from the much larger free energy of binding and from viscosity measurements indicating substantial lengthening.[24] Barton et al. also conclude that intercalation of DPPZ be a likely explanation of the unwinding and spectacular increase in luminescence of [Ru(phen)$_2$(DPPZ)]$^{2+}$ upon binding DNA.[8,25] From the observation of several lifetimes exhibited by methylated DPPZ complexes, it has been speculated that there are two distinct orientations (one symmetric and one skewed) of the DPPZ wing within the intercalation pocket.[30] Since LD can probe orientations relative to the helix axis only, we do not address this proposal about heterogeneity. We observe that the C_2 axis of the complex is perpendicular to the helix axis and thus find it natural to discuss our results in terms of the high-symmetry geometry in which the C_2 axis of the complex coincides with the pseudo-dyad axis of DNA.

Diastereomeric Binding Geometries. Of any electronic spectroscopic technique, linear dichroism spectroscopy most distinctly shows up diastereomeric effects of ruthenium complexes upon interaction with DNA.[23,28,42] The Λ enantiomers, when bound to flow-oriented DNA, invariably show a much more positive LD near the MLCT-band center (420 nm) than their Δ counterparts. Binding to DNA also induces noticable changes in the CD spectra of ruthenium complex enantiomers,[22,28,43] but the structural implications here are less clear-cut due to the strong inherent CD which is not yet completely understood. Differences in normal (isotropic) absorption spectra between pairs of DNA-bound enantiomers are in general quite small, although there is a clear trend for slightly more hypochromism in the MLCT band of Δ complexes. The linear dichroism spectrum, when normalized with respect to orientation of DNA, is directly related to the angles $\theta(i)$ that the individual transition moments i (with absorbance ϵ_i) of the complex make with the helix axis (eqs 7 and 9). The differences between the enantiomers are thus direct consequences of the diastereomeric binding geometries of the complexes.

It is instructive to consider the metal complex as composed of one *symmetric* and one *dissymmetric* part, *viz*., the ligand containing the C_2 axis (*i.e*., DPPZ) and the two phenanthroline "propeller blades". Only the latter, dissymmetric part can give rise to diastereomeric interaction. The orientation of the complex around the C_2 axis (roll angle β) will modulate this interaction. For example, for Δ-[Ru(phen)$_2$(DPPZ)]$^{2+}$, β = +10° would permit the propeller blades to have their longest dimension parallel to the groove and thereby minimize the radial distance to the helix center (maximum penetration). For the Λ enantiomer, β would have to be +80° for such an arrangement and since this is, of course, impossible with DPPZ intercalated, this represents one determinant of chiral discrimination.

However, neither the geometries nor the thermodynamic stabilities[24] indicate any drastic structural or thermodynamic differences between the DNA adducts with the two enantiomers of [Ru(phen)$_2$(DPPZ)]$^{2+}$. Differences are mainly manifest in the optical properties, on one hand as a consequence of

(41) Dupureur, C. M.; Barton, J. K. *J. Am. Chem. Soc.* **1994**, *116*, 10286.

(42) Yamagishi, A. *J. Chem. Soc., Chem. Commun. A* **1983**, 572. Yamagishi, A. *J. Phys. Chem.* **1984**, *88*, 5709.

(43) Nordén, B.; Patel, N.; Hiort, C.; Gräslund, A.; Kim, S. K. *Nucleotides and Nucleosides* **1991**, *10*, 195−205.

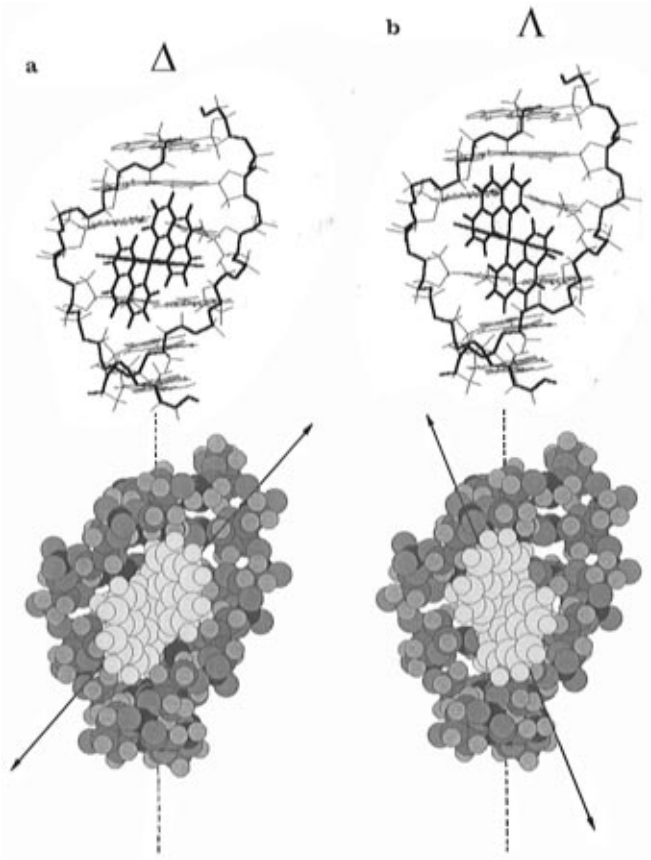

Figure 6. Models illustrating the diastereomeric binding geometries of the $[Ru(phen)_2L]^{2+}$ complexes with L = DPPZ and BDPPZ being intercalated and oriented perpendicular to the DNA helix axis (the complex is here placed in the minor groove). For both enantiomeric forms the spectroscopic results show the complex to be tilted from the idealized intercalative geometry by a *clockwise* roll around its C_2 axis (=long axis of L) with a roll angle of about 10°. The helix axis is shown with a dotted line and the direction of B(E) polarization as a double-headed arrow. The models were generated from a molecular mechanics energy minimization (Amber force field in the HyperChem package).

diastereomeric orientation effects of the chromophore (seen in LD) and on the other as a consequence of different penetrations (seen in emission and hypochromicity). At the same time, the obvious difference in fitting between the two phenanthroline propeller blades and the DNA strands (Figure 6) suggests that, although the actual variations in binding thermodynamics appear to be rather subtle in this particular case, the machinery for enantiomeric selection is there.

Roll Angle. If the roll angle β had been exactly zero for $[Ru(phen)_2(DPPZ)]^{2+}$, the angle between the B(E) polarized transition moments and the DNA axis should have been +35° and −35° for the Δ and Λ enantiomers, respectively. Since LD depends on cosine squared, this would have resulted in identical LD spectra for the two enantiomers. Hence, the observation of markedly different LD spectra for Δ- and Λ-$[Ru(phen)_2(DPPZ)]^{2+}$ immediately implies a non-zero roll for at least one of the enantiomers.

An approximate "reflection symmetry" between the LD^r and FA profiles (Figure 4a) of Δ-$[Ru(phen)_2(DPPZ)]^{2+}$ must be due to the helix axis of DNA roughly bisecting the angle between the two major transition moments, B(E) and $B(A_2)$, that are perpendicular to the C_2 axis. This rather fortuitous circumstance enables quite accurate determination of the roll angle for the Δ-$[Ru(phen)_2(DPPZ)]^{2+}$ complex (Table 2). The sign of the roll is unambiguously determined due to the identification of a B(sh) transition with strongly negative LD. For Λ-$[Ru(phen)_2(DPPZ)]^{2+}$, the roll angle was determined assuming a negligible A_2 intensity in the low-energy part of the MLCT absorption region, which is justified by the polarized crystal spectra[38] of $Ru(bipy)_3^{2+}$ and the INDO calculations.

As seen in Table 2, the roll angles are of similar magnitude and *are all positive*. An apparent paradox with regard to the large differences in the LD spectra mentioned above is presented by the very similar roll angles for the two enantiomers. The explanation is that a clockwise roll will correspond to directions of the B(E)-polarized intensity at the angles $(35° + \beta)$ for Δ enantiomers and $-(35° - \beta)$ for Λ, relative to the helix axis. This difference of 2β, in the case of identical *intercalation* geometries of the two enantiomers, thus leads to different LD spectra. The LD difference is merely a consequence of the spectroscopic diastereomerism due to the different orientations of the *dissymmetric* part, the two phenanthroline propeller blades, relative to the DNA helix axis, as illustrated in Figure 6.

The fact that we obtain angles around +10° for all $[Ru(phen)_2(DPPZ)]^{2+}$-like derivatives studied, with the plus sign meaning a clockwise roll when viewing toward the DNA, indicates a significant deviation in this direction, either imposed by the intercalator complex or due to a tilt of the nucleo-bases which is intrinsic to the DNA structure. In this context it can be recalled that LD^r of the DNA bases (indirectly determined with the methylene blue reference) was less negative than for the A-polarized transitions. The difference corresponds to a base tilt of 17° ± 2° in fair agreement with the 10−20° suggested from other studies (e.g. a tilt by 20° of the long axis of the base-pair pocket was indicated from the different LD^r values of short- and long-axes-polarized transitions of intercalated quinacrine).[27] If our roll thus reflects the native solution structure of B-DNA we have also determined in which direction the nucleo-bases are tilted, provided we can settle whether the complex is bound via the minor or major groove. Based on earlier mentioned inferences, we have tentatively placed the complex in the minor groove in the model calculation shown in Figure 6. The clockwise roll is clearly seen by the tilt of the intercalating (B)DPPZ ligand in the top panels for both enantiomers, whereas the different orientations of the phenanthroline pair are shown in the bottom panels: pointing along the groove for Δ and toward the wall of the groove for Λ.

We notice a striking similarity between the binding geometry concluded for Δ-$[Ru(phen)_2(DPPZ)]^{2+}$ and that of actinomycin D as found in the first crystal structure of a larger intercalator in a long DNA sequence.[44] Actinomycin D is present in the enantiomeric form that corresponds to the Δ enantiomer of $[Ru(phen)_2(DPPZ)]^{2+}$. Furthermore, it has one planar aromatic three-ring system which is intercalated and two peptide propeller wings that correspond to the symmetric (DPPZ) and dissymmetric (the two phens) moieties of $[Ru(phen)_2(DPPZ)]^{2+}$. Actinomycin binds from the minor groove, and steric interference of the peptide chelate wings gives rise to a distinct bend of the helix. It is interesting to note here that while the Λ form of $[Ru(phen)_2DPPZ]^{2+}$ gives rise to a significant increase in DNA orientation, as may be expected for an intercalator that extends the length of DNA, the Δ enantiomer has very little effect. In view of the actinomycin−DNA structure this could be a result of a counteracting effect of a bend that the Δ complex, but not to the same extent the Λ complex, induces upon binding to DNA.

Error Analysis. The approximate mirror image relationship between EA and LD^r for Δ-$[Ru(phen)_2DPPZ]^{2+}$ bound to DNA allows in this case a rather precise determination of the value

(44) Kamitori, S.; Takusagawa, F. *J. Am. Chem. Soc.* **1994**, *116*, 4154.
(45) Braddock, J. N.; Meyer, T. J. *J. Am. Chem. Soc.* **1973**, *95*, 3158.

of $\theta_{B(E)}$ to 42 ± 3° but gives no further information regarding the spectral overlap of B(E) and B(A_2) transitions. The value of $\theta_{B(E)}$ for the Λ complex is thus strongly dependent on the assessment of this overlap, and the value of −22° ± 5° was estimated assuming an as small as possible long-wavelength contribution for the B(A_2) component. Although the INDO/S calculations, and polarized crystal spectra of the parent chromophore [Ru(bipy)$_3$]$^{2+}$, support this assumption, we cannot rigorously exclude that $\theta_{B(E)}$ for Λ is closer to zero, and the roll angle β for the Λ enantiomer is correspondingly larger. Further, the calculation of the roll angles from the values of $\theta_{B(E)}$ introduces an error due to the necessarily approximate nature of the calculation of the direction of the B(E) transition moments. However, as the qualitative treatment of the perturbation of the parent D_3 chromophore indicates, this error will be relatively small. Finally, even if there were a relatively large error in the direction of the B(E) transition moment in the chromophore framework, the sum of the roll angles $\beta(\Delta) + \beta(\Lambda)$ would still remain rather precisely determined to about 20° ± 5°.

Electronic Transitions. To extract exact geometric information, both the polarizations of the transitions within the complex and the extent of overlap of differently polarized absorption bands had to be determined. A first important observation, that the replacement of one phen in [Ru(phen)$_3$]$^{2+}$ by a DPPZ ligand only slightly perturbs the symmetry of the MLCT chromophore, is made both from the molecular orbital calculations (transition energies and total oscillator strengths in Table 1) and the CD results (see Experimental). Since CD is very sensitive to transition moment directions, the similar CD spectra of [Ru(phen)$_3$]$^{2+}$ and [Ru(phen)$_2$(DPPZ)]$^{2+}$ therefore indicate very similar polarizations when regarded in D_3 symmetry. This observation justifies the simple vectorial A + B decomposition of the E transition moments, upon lowering the symmetry to C_2 for the analysis of the LD spectrum of the oriented chromophore. This approach is also supported by the small splitting between the A and B components as predicted by the molecular orbital calculations, although a somewhat larger intensity was obtained for the A than for the B component upon DPPZ substitution.

In view of the complex nature of the MLCT system, the agreement between predicted and experimental spectra must be considered as very good. (The agreement regarding position and polarization of the first intraligand $\pi \rightarrow \pi^*$ transition is excellent.) The presence of the four effective transition moment directions (Figure 1 and 5) is in essence confirmed by the calculations for energies below 33 × 10^3 cm^{-1} (wavelengths above 300 nm). The goodness of the calculation is also indicated by the correct prediction of an overall E-polarized intensity in the low-energy MLCT region, with elements of A_2 polarization occurring first at higher energy, in perfect agreement with polarized crystal spectra.[38] Note thus, that our previous analysis of flow LD spectra of [Ru(phen)$_3$]$^{2+}$ bound to DNA involved an incorrect assignment by assuming an A_2 component at the red edge of the MLCT absorption band leading to an erronous conclusion about the orientation of the complex; a separate study will be devoted to DNA binding geometries of [Ru(phen)$_n$(bpy)$_{(3-n)}$]$^{2+}$ complexes (Lincoln, Tuite, and Nordén, to be published).

Conclusions

Our study represents a rare situation in which it has been possible to analyze a complicated three-dimensional chromophore with respect to transition moment directions and mutual overlap of absorption. In turn, the transition moment data have allowed relatively precise determination of angles of four principal transition moment directions in the [Ru(phen)$_2$L]$^{2+}$ complex ions characterizing the DNA binding geometry. Four important conclusions emerge:

1. The plane of the DPPZ (and BDPPZ) chelate ligand as characterized by several angles is oriented near parallel with the nucleo-base planes as expected if this ligand is intercalated. That this chelate ligand is not turned away from DNA (the alternative solution) is proven by the strong hypochromicity of the intraligand transition evidencing close contact with nucleobases.

2. The markedly different LD spectra of the Δ and Λ forms of either of the two studied complexes is an effect of a small but distinct inclination ("roll") of the complex around the long axis of the intercalated (B)DPPZ wing (approximately a dyad axis of DNA). The LD of the B(E) MLCT transition is concluded to be a sensitive indicator, depending on the direction of roll and the enantiomeric form of complex.

3. The roll is in the same direction (clockwise) for both enantiomers and it varies relatively little between the DPPZ and BDPPZ complexes or with DNA sequence. The inclination may be intrinsic to DNA, in which case it corresponds to a clockwise tilt of bases around the pseudo-dyad axis, or it may represent a conformational distortion induced upon binding of the metal complex.

4. The binding geometry concluded for Δ-[Ru(phen)$_2$DPPZ]$^{2+}$ shows similarities to the crystal structure of actinomycin D bound to a long DNA sequence, including the intercalation, the positioning of the "propeller blades", and also the clockwise inclination. A bending of the DNA may also be a common factor that could explain the impaired flow-orientation of DNA when interacting with the Δ compared to the Λ complex ion.

Acknowledgment. Dr. Bo Albinsson is gratefully acknowledged for inspiring the authors to use emission anisotropy. This project was funded by the Swedish Natural Science Research Council (NFR).

JA953363L